BIOCHEMISTRY

 Volume 44, Number 32 August 16, 2005

Articles

Foldamers with Hybrid Biological and Synthetic Sequences as Selective DNA Fluorescent Probes†

Wei Wang, Wei Wan, Andrew Stachiw, and Alexander D. Q. Li*

Department of Chemistry, Washington State University, Pullman, Washington 99164

Received May 23, 2005; Revised Manuscript Received June 16, 2005

ABSTRACT: Foldable polymers with alternating single-strand deoxyribonucleic acid (ssDNA) and planar fluorescent organic chromophores can self-organize into folded nanostructures and hence are hybrid foldamers with biological sequences and synthetic properties. The biological sequence provides highly specific molecular recognition properties, while the physical properties of synthetic chromophores offer sensitive fluorescence detection. In this paper, we describe that rational designed hybrid foldamers exhibit potential in the detection of polynucleotides. Under strictly controlled laboratory conditions, fluorescence measurements indicate that configuration change due to binding of polynucleotides with one or two mismatched bases can be readily distinguished. These results shed light on the design and construction of nanostructured foldamers with actuator and sensory properties, which may find important applications as biological probes.

Detection of DNA has attracted great interest recently, especially in the area of applying emerging nanotechnology (*1*−*3*) to biotechnology (*4*−*6*). The advantages of integrating nano-biotechnology are that biological macromolecules such as DNA offer specific interaction whereas nanoparticles provide a means of amplification of such molecular recognition events. Typically, a DNA macromolecule binds to its complementary strand in a subtle way that is different from that of mismatched strands (*7*, *8*). When such subtle discrimination is amplified, a potential viable DNA detection mechanism is developed. One way to amplify such molecular recognition events is to use the size-dependent dielectric properties of gold nanoparticles (*9*, *10*). Another is utilization of fluorescent properties of either nanoparticles or organic chromophores and their sensitivity to distance and size (*11*). Herein, we demonstrate that folding and unfolding of a hybrid polymer containing alternating biological sequences and synthetic chromophores with orthogonal fluorescence emissions can be applied to DNA detection.

Our general strategy for developing foldable polymers is to alternate a hydrophobic sequence and a hydrophilic sequence in a controlled placement and orientation with a single molecular weight distribution. Highly fluorescent chromophores are embedded in the hydrophobic sequences; quantum interactions between these chromophores, such as π-orbital overlap and resonance energy transfer, are very sensitive to their distance separation, thus providing a means of gauging folding and unfolding events. Fluorescence resonance energy transfer (FRET)[1] between chromophores in the processes of folding or unfolding is particularly interesting because it can be amplified by distance change; even single molecular events could be monitored with fluorescence (*12*−*16*). The typical requirements for the hydrophilic sequences in foldable polymers are flexibility

† We acknowledge the support of the National Institute of General Medical Sciences (Grant 065306) and the Arnold and Mabel Beckman Foundation. A.D.Q.L. is a Beckman Young Investigator (BYI).

* To whom correspondence should be addressed: Department of Chemistry, Washington State University, Pullman, WA 99164. Telephone: (509) 335-7196. Fax: (509) 335-8867. E-mail: dequan@wsu.edu.

10.1021/bi050945z CCC: $30.25
Published on Web 07/22/2005

and solubility. Both characteristics are important because flexibility provides hingelike function, allowing the hydrophobic chromophores to fold, while solubility is needed for the studies of individual folded nanostructures in solution. Yet, more importantly, if the flexible sequences exhibit exquisite molecular recognition properties, then molecular recognition-induced folding and unfolding events can trigger a sensitive change in the quantum interactions among chromophores (*17*−*19*). An ideal hydrophilic sequence that satisfies all these requirements is the macromolecule used for genetic codes, single-strand DNA.

EXPERIMENTAL PROCEDURES

Synthesis of DDP. DDP was synthesized by condensing 2,6-dimethyl-4-(dicyanomethylene)pyran with a slight excess of 4-*N*-*n*-butyl-*N*-(2-{2-[2-(2-hydroxyethoxy)ethoxy]ethoxy}-ethyl)aminobenzaldehyde in the presence of piperidine catalyst and purified using chromatography. The purified DDP was monotritylated by reaction with 3 equiv of dimethoxy trityl chloride at room temperature. The monotritylated product was purified on a silica column and verified with ^{1}H NMR and mass spectrometry. ^{1}H NMR ($CDCl_3$): δ 7.49−7.38 (m, 8H, aromatic rings and double bond trans-linkage), 7.34 (dt, 4H, $J_1 = 2.7$ Hz, $J_2 = 9$ Hz, methoxylbenzene ring), 7.31−7.15 (m, 3H, benzene ring), 6.81 (dt, 4H, $J_1 = 2.7$ Hz, $J_2 = 9$ Hz, methoxylbenzene ring), 6.69 (d, 2H, $J = 8.7$ Hz, benzene ring), 6.66 (d, 2H, $J = 9.0$ Hz, benzene ring), 6.54 (d, 1H, $J = 2.1$ Hz, pyran ring), 6.52 (d, 1H, $J = 2.1$ Hz, pyran ring), 6.48 (d, 1H, $J = 15.9$ Hz, double bond trans-linkage), 6.46 (d, 1H, $J = 15.9$ Hz, double bond trans-linkage), 3.77 (s, 6H, CH_3O), 3.56−3.50 (m, 30H, tetraethylene glycol chain), 3.44−3.31 (m, 4H, *n*-butyl chain), 3.22 (t, 2H, $J = 5.1$ Hz, tetraethylene glycol chain), 1.69−1.49 (m, 4H, *n*-butyl chain), 1.48−1.42 (m, 4H, *n*-butyl chain), 0.97 (t, 3H, $J = 7.5$ Hz, *n*-butyl chain), 0.96 (t, 3H, $J = 7.5$ Hz, *n*-butyl chain). ^{13}C NMR ($CDC1_3$): δ 159.5, 158.4, 156.2, 149.8, 145.1, 138.2, 136.4, 130.2, 129.9, 128.3, 127.8, 126.7, 122.2, 122.1, 116.5, 113.1, 112.94, 112.88, 111.8, 111.7, 105.4, 86.1, 72.7, 71.0, 70.92, 70.84, 70.76, 70.5, 68.6, 63.3, 61.9, 56.1, 55.4, 51.4, 50.6, 29.4, 20.5, 14.3. MS (ESI): m/z 1145.6 $[M]^+$. The characterized monotritylated product was treated with a slight excess of chloro-*N*,*N*-diisopropylaminocyanoethoxyphosphane to yield the desired phosphoramidite of DDP.

Synthesis of HSB. HSB was synthesized by reacting a Wittig reagent tetraethyl 1,4-xylylenediphosphonate (1.05 g, 2.78 mmol) with 3 equiv of 4-(2-{2-[2-(2-hydroxyethoxy)-ethoxy]ethoxy}ethoxy)benzaldehyde. The purified HSB was monotritylated using a procedure similar to that for DDP, and the tritylated product was purified with a silica column and extensively characterized with NMR. ^{1}H NMR ($CDCl_3$): δ 7.46 (s, 4H, aromatic ring of styryl benzene), 7.49−7.38 (m, 6H, aromatic rings of styryl benzene and DMTr), 7.34 (dt, 4H, $J_1 = 8.7$ Hz, $J_2 = 2.3$ Hz, methoxylbenzene ring), 7.31−7.15 (m, 3H, benzene ring of DMTr), 7.06 (d, 1H, $J = 16.2$ Hz, double bond trans-linkage), 7.05 (d, 1H, $J = 16.2$ Hz, double bond trans-linkage), 6.96 (d, 1H, $J = 16.2$ Hz, double bond trans-linkage), 6.95 (d, 1H, $J = 16.2$ Hz, double bond trans-linkage), 6.94−6.84 (m, 4H, aromatic ring of styryl benzene), 6.81 (dt, 4H, $J_1 = 8.7$ Hz, $J_2 = 2.3$ Hz, methoxylbenzene ring), 4.19−4.08 (m, 4H, tetraethylene glycol chain), 3.89−3.82 (m, 4H, tetraethylene glycol chain), 3.80−3.58 (m, 28H, CH_3O and tetraethylene glycol chain), 3.22 (t, 2H, $J = 5.1$ Hz, DMTrOCH_2). ^{13}C NMR ($CDC1_3$): δ 158.57, 158.55, 158.43, 145.2, 136.74, 136.70, 136.4, 130.47, 130.40, 130.2, 128.3, 128.00, 127.96, 127.87, 127.79, 126.77, 126.67, 126.44, 126.38, 115.0, 113.2, 86.1, 72.7, 71.09, 71.04, 70.98, 70.95, 70.88, 70.81, 70.56, 69.95, 67.64, 63.4, 62.0, 55.4. The phosphoramidite was obtained by reacting the monotritylated product with ∼2 equiv of chloro-*N*,*N*-diisopropylaminocyanoethoxyphosphane and used immediately on the solid-state synthesizer.

Synthesis and Purification of Hybrid Foldamers with Alternating Fluorescent Chromophores and Oligonucleotide DNA. Since the coupling reactions of the fluorescent emitters on the automated DNA synthesizer had been optimized and were compatible with phosphoramidite chemistry used in DNA synthesis, the insertion of the two chromophores described above via tetraethylene glycol spacer phosphoramidites into the designed DNA sequences during DNA chain growth was successfully completed on an Expedite 8900 Nucleic Acid Synthesis System.

The detailed protocol of solid-phase synthesis of foldamers was reported previously (*17*), and here we simply summarize the key parameters. The DDP and HSB phosphoramidite reagents were prepared in dichloromethane because they have low solubility in the "standard" solvent of the synthesizer acetonitrile. The concentration of DDP and HSB phosphoramidite was ∼100 mg/mL, and their coupling reaction time on the solid-phase columns were extended to ∼30 min to achieve high coupling yields. Reaction parameters of other steps (oxidation and detritylation) on the solid-phase columns are similar to what was used for DNA synthesis.

The Oligonucleotide Purification Cartridge (ABI Masterpiece) was used to purify the obtained crude oligonucleotides with the terminal DMTr group. With high coupling yield during foldamer chain assembly (>80−99% based on trityl monitor) and good overall yield, the OPC (Oligonucleotide Purification Cartridge)-purified foldamers could be used for DNA detection after desalting. A typical procedure follows.

After solid-state synthesis, the column containing 0.2 μmol of the designed foldamer is removed from the DNA synthesizer. A syringe is attached to each end of the column, one syringe containing 1 mL of fresh ammonium hydroxide (NH_4OH, 29% w) and the other empty. The ammonium hydroxide solution is injected through one end of the column and forced through the column by depressing the syringe, and simultaneously collected in the empty syringe attached on the opposite end of the column. After all the ammonium hydroxide solution has been passed through the column, the solution collected in the opposite syringe is then forced back through the column. Again the solution is collected in the original syringe. This "extraction" process is repeated three or four times to ensure that the support in the column is

[1] Abbreviations: FRET, fluorescence resonance energy transfer; DMTr, dimethoxy trityl; OPG, oligonucleotide purification cartridge; ODU, optical density unit, which is equivalent to an absorbance unit (AU); RT, room temperature; HPLC, high-performance liquid chromatography; TEAA, triethylammonium acetate; TEG, tetraethylene glycol; DDP, 2,6-diaminostyryl 4-dicyanomethylene-4*H*-pyran; HSB, 1,4-[bis-4,4′-(2-{2-[2-(2-hydroxyethoxy)ethoxy]ethoxy}ethoxy)styryl]-benzene; BYB, blue−yellow−blue [foldamer]; OM1, one-mismatch [sequence] 1; OM2, one-mismatch [sequence] 2; TM1, two-mismatch [sequence] 1; TM2, two-mismatch [sequence] 2.

fully saturated. The column−syringe assembly is allowed to rest at RT for 1 h, and the extraction process is repeated another three or four times. After the column−syringe assembly has been allowed to rest once more at RT for an additional 1 h, the solution is drawn completely into one syringe, which is then carefully removed from the column. The solution is then delivered into a 10 mL flask with a sealed septum and a stir bar. After it has been stirred for 48 h at RT, 20 μL of the solution is diluted with 3000 μL of distilled water, and the optical density unit (ODU) value, which is equivalent to an absorbance unit, of this solution is measured at 260 nm. On the basis of the ODU value, the original ammonium hydroxide solution is diluted so that the final ODU value is <10. The foldamer purification is then carried out according to the protocol provided by ABI Masterpiece (2 mL diluted solution with ODU ≤ 10 for each OPC column). The OPC purified trityl-off foldamers are stored as a dry solid at −80 °C. According to the desalting protocol provided by ABI Masterpiece, the trityl-off foldamers are dissolved in water (1 mL), and the resulting solution is passed through another activated OPC column, at last collected with 1 mL of a 50% acetonitrile/water solution. The obtained acetonitrile/water solution is then concentrated to dryness in a vacuum, and the salt-free foldamer is obtained as a solid, which can be stored at −20 °C for further studies. This completes the crude separation of foldamers, and they are further purified via HPLC as described below.

HPLC Purification of Oligo DNA and the Hybrid Foldamers. The oligo DNA 18-mers were purified using an ion-exchange column (Zorbax Oligo; 5 μm). The mobile phase consists of two buffers, and a linear salt gradient is used to elute the DNA samples. The first buffer contains 20% acetonitrile and 80% water (v/v) with 0.01 M NaH_2PO_4 and 0.01 M Na_2HPO_4 to ensure the pH equals 7. The second buffer has 2 M NaCl dissolved in the first buffer. The desired oligo DNA is eluted by increasing the salt gradient, and the samples are >95% pure.

The hybrid foldamer is purified using a Genesis 300 C4 (4 μm) reverse-phase column. A linear gradient is used with an increasing organic component to elute the desired hybrid foldamer. The aqueous buffer contains 0.1 mM triethylammonium acetate (TEAA) in filtered milli-Q water. The organic buffer contains 0.1 mM triethylammonium acetate (TEAA) in HPLC grade acetonitrile. A typical run will start with high aqueous buffer composition and slowly ramp up the organic buffer to elute the desired foldamer. The final foldamer is >95% pure.

Fluorescence Measurements. Fluorescence measurements were carried out on a SPEX Fluorolog-3-21 instrument. A typical experiment uses a 10 nM solution of the hybrid foldamer in a 1 mL quartz cell, and the sample is excited at 365 nm. Sequences of DNA with the complementary structure or various mismatches are then added to the sample cell after the fluorescence intensity is initially read. The fluorescence spectra of various samples with reduced fluorescence resonance energy transfer (FRET) efficiency are collected.

For kinetics experiments, the fluorescence intensity versus time curve is recorded and the folded concentration is calculated using the fluorescence intensity of the FRET peak. The data are then fitted into a first-, second-, or third-order kinetics equation, and the rate constants are obtained from the slope of the straight lines. All samples used in kinetics measurements are purified with HPLC and used immediately after the purified sample is dissolved in autoclaved water.

RESULTS AND DISCUSSION

To construct foldable polymers with alternating hydrophobic and hydrophilic structures, we employed solid-phase synthesis (*20*, *21*), which requires that the fluorescent building blocks have an activated functional group for attachment to the growing end of the DNA polymer chain and a removable protecting group so that it can be removed to permit further chain extension (*22*). Two fluorescent chromophores are synthesized: one emits in the yellow with a λ_{max} of ∼612 nm, and the other emits in the blue with an emission maximum at 480 nm in organic solvents. In addition to their fluorescence emission, the absorption maximum of the yellow chromophore (486 nm) overlaps perfectly with the fluorescence emission of the blue chromophore. The yellow emitter is based on the 2,6-diaminostyryl 4-dicyanomethylene-4*H*-pyran or DDP structure (Figure 1a). Flexible tetraethylene glycol (TEG) linkers (*23*) were attached to both amino groups of DDP, yielding two hydroxyl groups at either end of the chromophore. One hydroxyl group was protected with a removable blocker, a dimethoxy trityl (DMTr) group, and the other was activated with a phosphoramidite group. The blue emitter is 1,4-[bis-4,4′-(2-{2-[2-(2-hydroxyethoxy)ethoxy]ethoxy}ethoxy)styryl]benzene (HSB), and it is similarly functionalized with removable DMTr protection and an active phosphoramidite for efficient coupling to hydroxyl groups.

Solid-phase DNA synthesis is well developed (*21*). Synthesis of hybrid oligonucleotides containing stilbene units is also reported with a satisfactory yield (*24*, *25*). However, general incorporation of organic chromophores into DNA main chains is still not trivial (*26*, *27*) and frequently requires special manipulation (*28*, *29*). Rarely, more than two chromophores are incorporated into DNA main chains due to limited synthetic yields. Herein, the incorporation of two HSB and one DDP chromophore into the DNA backbone is achieved in high yield by repeating the coupling reaction. The foldable polymers synthesized on solid supports are purified using HPLC (Genesis 300, C_4 column) to yield >95% pure samples. The foldable polymer for this study has a sequence of DNA-HSB-DNA-DDP-DNA-HSB-DNA, where HSB and DDP are the two fluorescent segments and DNA has a base sequence of 5′-ATC-CGG-AGT-CAG-CCG-GAT-3′ except the terminal DNA sequence which has been truncated after two AT bases (Figure 1b,c). The above foldamer is named BYB because of an alternating blue−yellow−blue fluorescent sequence.

In aqueous solutions (pH ∼5), HSB and DDP in BYB fluoresce at 435 and 545 nm, respectively. The shifts in fluorescence emissions are attributed to the change in solvent and pH effects on chromophores. The purified BYB sequence forms the predominately folded structure, in which the two chromophores are in approximately juxtaposed positions. Since the emission bands of HSB overlap strongly with the absorption band of the DDP, fluorescence resonance energy transfer (FRET) will quench the blue emitter and yellow emission will dominate the fluorescence spectrum. Indeed,

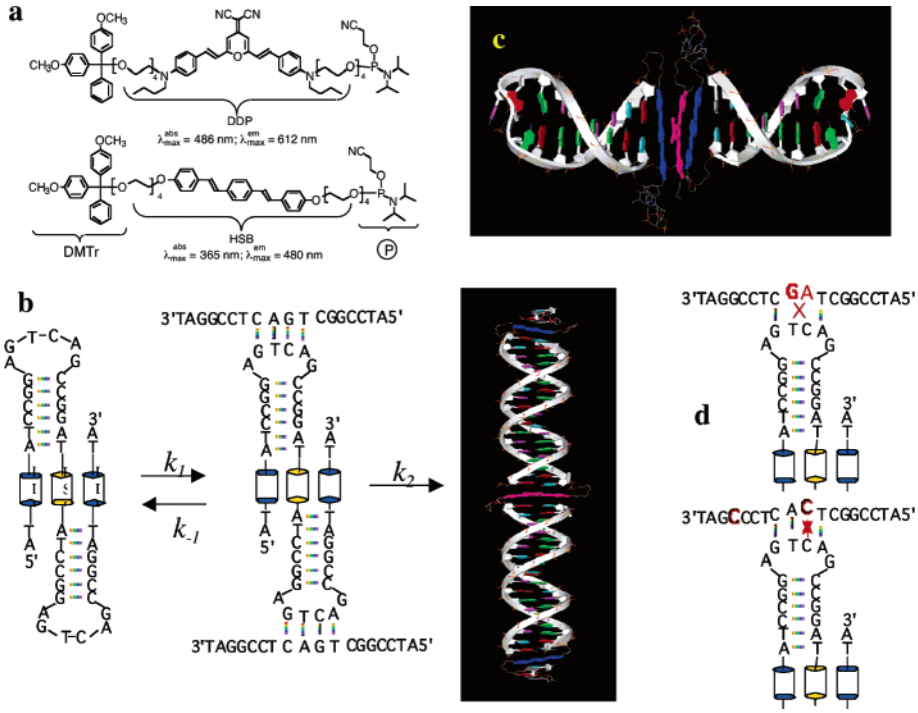

FIGURE 1: (a) Chemical structures of the two fluorescent chromophores (HSB and DDP), modified with a removable DMTr protecting group and an activated phosphoramidite group. (b) Foldamer BYB sequence and its reaction with the complementary DNA sequence. (c) Model of the folded molecular structure. (d) Mismatched sequences do not form supramolecular assemblies.

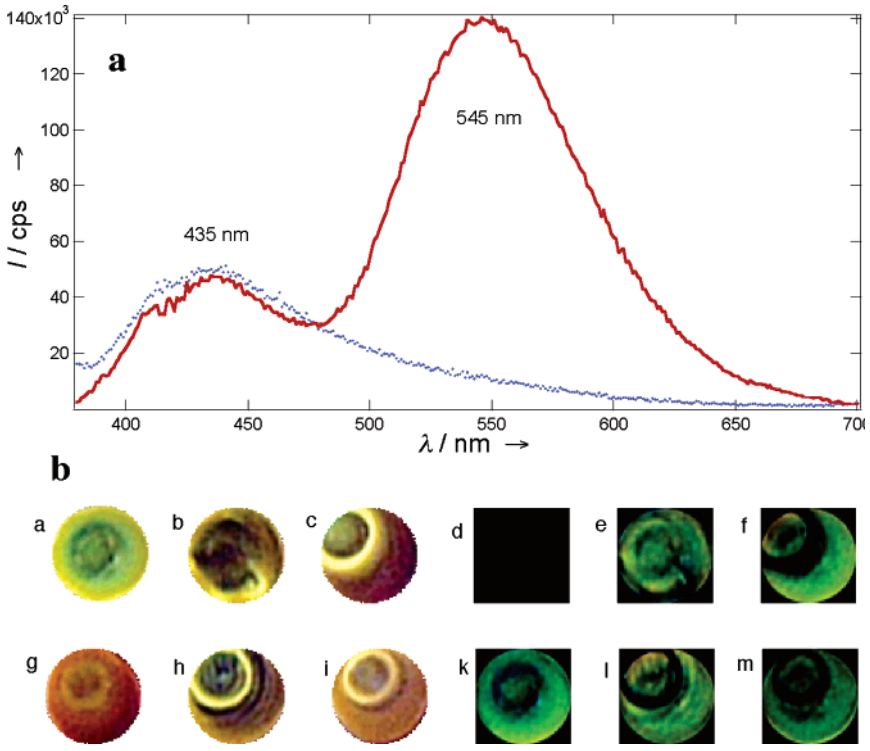

FIGURE 2: (a) Fluorescence spectra show that folded BYB (10 nM) emits dominantly at 545 nm (line). Once it binds to the complementary strand, the fluorescence resonance energy transfer efficiency drops significantly between HSB and DDP chromophores and the unfolded BYB fluoresces at 435 nm (dots). (b) Comparison of fluorescence colors of foldamers binding to the perfect match (a), one-mismatch forms [OM1 (b) and OM2 (c)], two-mismatch forms [TM2 (h) and TM1 (i)], and blank (g). The perfect match generates a green spot (a), whereas a pure foldamer yields an orange spot (g). The difference in the colors is presented between perfect match with perfect match (d), OM1 (e), OM2 (f), blank (k), TM1 (m), and TM2 (l).

this behavior was observed (Figure 2a and image g of Figure 2b).

Subsequently, the BYB foldamer was exposed to various oligonucleotides, having either the complementary sequence or various mismatched base pairs to the DNA in BYB (Table 1). To evaluate the feasibility that the foldamer can discriminate perfect match strand from those mismatched strands, 2 μL ($\sim$9.2 pmol) of the reaction solution was condensed on glass slides to dryness. The resulting fluorescence spots on glass have enough color differences to allow

Table 1: Various DNA Sequences Used To Probe BYB Foldamer Responses

name	DNA sequence
complementary	3′-TAG-GCC-TCA-GTC-GGC-CTA-5′
OM1	3′-TAG-GCC-TC**T**-GTC-GGC-CTA-5′
OM2	3′-TA**C**-GCC-TCA-GTC-GGC-CTA-5′
TM1	3′-TAG-**C**CC-TCA-**C**TC-GGC-CTA-5′
TM2	3′-TAG-GCC-TC**G**-**A**TC-GGC-CTA-5′

Table 2: Normalized Fluorescence Intensities of the Yellow Fluorescence Band at 545 nm at Various Reaction Times[a]

reaction time (min)	complementary	OM1	OM2	TM1	TM2
30	0.79	0.93	0.99	0.97	0.99
60	0.55	0.89	0.96	0.92	0.97
90	0.41	0.83	0.95	–	–

[a] The complementary strand is very efficient at unfolding the BYB foldamer and hence produces the largest reduction of the yellow fluorescent band.

visual identification of the perfect match from those having one or two mismatched bases.

Two sequences with one-base mismatch were studied, and the mismatched base was introduced either in the middle of (OM1) or toward the end of the oligonucleotide (OM2). Both sequences with one base mismatch react with BYB, yielding yellow or yellow green fluorescent spots (Figure 2b, images b and c). The reaction between BYB and its complementary sequence yields green fluorescent spots (Figure 2b, image a). The color difference between perfect match and the two one-mismatch sequences is distinguishably green (Figure 2b, images e and f), whereas perfect match against perfect match in control experiments yields a black background (Figure 2b, image d).

Similarly, two sequences with a two-base mismatch were also investigated; the first sequence has a mismatch in the middle and another toward the end of the sequence (TM1), while the second sequence has two positionally switched bases in the middle. Both TM1 and TM2 have considerable yellow fluorescence emissions (Figure 2b, images h and i). Therefore, the difference in color between the perfect match and TM1 and TM2 is vividly green (images l and m). These results indicate that sequences with more than one base mismatch (TM1 and TM2) can be readily distinguished.

Quantitative fluorescence changes due to unfolding of the BYB foldamer are listed in Table 2 for complementary target DNA along with the mismatched sequences. At the 30 min reaction time, the perfect match reduces the fluorescence intensity at 545 nm by more than 20% while the mismatched sequences reduce the intensity by approximately 1−7%. At 60 min, the reaction of the complementary sequence is approximately halfway to completion while the mismatched sequences only finish 3−11%. These results are in agreement with the fluorescent color observed in Figure 2.

The origin of fluorescence color identification comes from differences in reactivity between the complementary strand and mismatched strands, which manifest in the kinetic studies. Figure 3 plots the kinetic data of the reaction between the BYB complementary oligonucleotide and sequences having mismatched bases. Although hybridization of complementary strands is not a unimolecular reaction, the rate law surprisingly fit better to a first-order reaction than to second- or third-order reactions with a first-order rate constant $k^{(1)}$ of $(1.00 \pm 0.02) \times 10^{-2}$ min^{-1}. This behavior is unexpected, indicating that the reaction pathway must have included a supramolecular intermediate species and the rate-determining step must be the unfolding of the supramolecular assembly (Figure 1b).

For one-mismatch sequences, kinetic data indicate the formation of a supramolecular complex is not the dominating

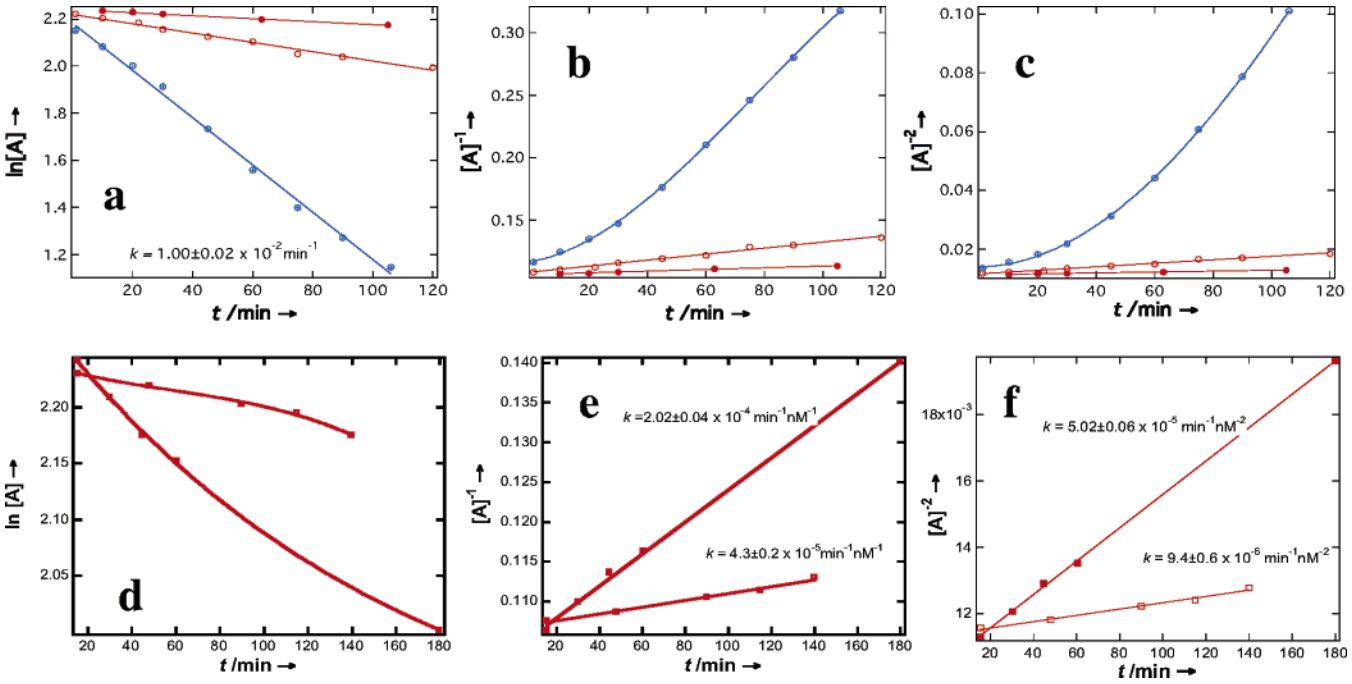

FIGURE 3: (a) Kinetics measurements of the rate constant for the reaction of BYB with the complementary oligonucleotide (⊕) yield a first-order reaction, whereas one-mismatch sequences [OM1 (○) and OM2 (●)] fit first-order, second-order (b), and third-order reactions (c). Two-mismatch sequences [TM1 (□) and TM2 (■)], however, no longer fit to the first-order reactions (d); instead, they fit to the second-order (e) and third-order reactions (f).

reaction pathway, whereas a supramolecular self-assembly is no longer the major reaction pathway for two-mismatch sequences (Figure 3d) because the fit to the first-order reaction is not a straight line. The second feature is that the reaction between complementary sequences is much faster than those of mismatched sequences. For OM1 and OM2 sequences, the rate constants for the first-, second-, and third-order reactions are as follows: $k^{(1)} = (1.99 \pm 0.09) \times 10^{-3}$ and $(6.3 \pm 0.3) \times 10^{-4}$ min^{-1}, $k^{(2)} = (2.40 \pm 0.01) \times 10^{-4}$ and $(6.9 \pm 0.3) \times 10^{-5}$ min^{-1} nM^{-1}, and $k^{(3)} = (5.9 \pm 0.2) \times 10^{-5}$ and $(1.53 \pm 0.05) \times 10^{-5}$ min^{-1} nM^{-2}, respectively. For TM1 and TM2 sequences, the rate constants for the second- and third-order reactions are as follows: $k^{(2)} = (4.3 \pm 0.2) \times 10^{-5}$ and $(2.02 \pm 0.04) \times 10^{-4}$ min^{-1} nM^{-1} and $k^{(3)} = (9.4 \pm 0.6) \times 10^{-6}$ and $(5.02 \pm 0.06) \times 10^{-5}$ min^{-1} nM^{-2}, respectively. All these rate constants are much smaller than that of the complementary strand, and therefore, the complementary polynucleotide yields more green to blue fluorescent spots than those of mismatched sequences.

In summary, we have demonstrated detection of single-nucleotide polymorphorism (SNP) using a hybrid foldamer at 1−10 nM. These results suggest foldamers with optimized structures should have potential application in DNA detection based on the sensitive switching of fluorescent colors. The simplicity of visual color change under UV radiation makes our foldamers attractive as DNA probes.

REFERENCES

1. Zhao, X. J., Tapec-Dytioco, R., and Tan, W. H. (2003) Ultrasensitive DNA detection using highly fluorescent bioconjugated nanoparticles, *J. Am. Chem. Soc. 125*, 11474−11475.
2. Maxwell, D. J., Taylor, J. R., and Nie, S. M. (2002) Self-assembled nanoparticle probes for recognition and detection of biomolecules, *J. Am. Chem. Soc. 124*, 9606.
3. Tyagi, S., and Kramer, F. R. (1996) Molecular beacons: Probes that fluoresce upon hybridization, *Nat. Biotechnol. 14*, 303−308.
4. Gaylord, B. S., Heeger, A. J., and Bazan, G. C. (2002) DNA detection using water-soluble conjugated polymers and peptide nucleic acid probes, *Proc. Natl. Acad. Sci. U.S.A. 99*, 10954−10957.
5. Patolsky, F., Lichtenstein, A., and Willner, I. (2001) Electronic transduction of DNA sensing processes on surfaces: Amplification of DNA detection and analysis of single-base mismatches by tagged liposomes, *J. Am. Chem. Soc. 123*, 5194−5205.
6. Dore, K., Dubus, S., Ho, H. A., Levesque, I., Brunette, M., Corbeil, G., Boissinot, M., Boivin, G., Bergeron, M. G., Boudreau, D., and Leclerc, M. (2004) Fluorescent polymeric transducer for the rapid, simple, and specific detection of nucleic acids at the zeptomole level, *J. Am. Chem. Soc. 126*, 4240−4244.
7. Ali, M. F., Kirby, R., Goodey, A. P., Rodriguez, M. D., Ellington, A. D., Neikirk, D. P., and McDevitt, J. T. (2003) DNA hybridization and discrimination of single-nucleotide mismatches using chip-based microbead arrays, *Anal. Chem. 75*, 4732−4739.
8. Gerion, D., Chen, F. Q., Kannan, B., Fu, A. H., Parak, W. J., Chen, D. J., Majumdar, A., and Alivisatos, A. P. (2003) Room-temperature single-nucleotide polymorphism and multiallele DNA detection using fluorescent nanocrystals and microarrays, *Anal. Chem. 75*, 4766−4772.
9. Elghanian, R., Storhoff, J. J., Mucic, R. C., Letsinger, R. L., and Mirkin, C. A. (1997) Selective colorimetric detection of polynucleotides based on the distance-dependent optical properties of gold nanoparticle, *Science 277*, 1078−1081.
10. Mitchell, G. P., Mirkin, C. A., and Letsinger, R. L. (1999) Programmed assembly of DNA functionalized quantum dots, *J. Am. Chem. Soc. 121*, 8122−8123.
11. Chakrabarti, R., and Klibanov, A. M. (2003) Nanocrystals modified with peptide nucleic acids (PNAs) for selective self-assembly and DNA detection, *J. Am. Chem. Soc. 125*, 12531−12540.
12. Tan, X., Hu, D. H., Squire, T. C., and Lu, P. (2004) Probing nanosecond protein motions of calmodulin by single molecule fluorescence anisotropy, *Biophys. J. 86*, 475A−475A.
13. Xie, Z., Srividya, N., Sosnick, T. R., Pan, T., and Scherer, N. F. (2004) Single-molecule studies highlight conformational heterogeneity in the early folding steps of a large ribozyme, *Proc. Natl. Acad. Sci. U.S.A. 101*, 534−539.
14. Bartley, L. E., Zhuang, X. W., Das, R., Chu, S., and Herschlag, D. (2003) Exploration of the transition state for tertiary structure formation between an RNA helix and a large structured RNA, *J. Mol. Biol. 328*, 1011−1026.
15. Schuler, B., Lipman, E. A., and Eaton, W. A. (2002) Probing the free-energy surface for protein folding with single-molecule fluorescence spectroscopy, *Nature 419*, 743−747.
16. Yang, H., Luo, G. B., Karnchanaphanurach, P., Louie, T. M., Rech, I., Cova, S., Xun, L. Y., and Xie, X. S. (2003) Protein conformational dynamics probed by single-molecule electron transfer, *Science 302*, 262−266.
17. Wang, W., Wan, W., Zhou, H.-Z., Niu, S., and Li, A. D. Q. (2003) Alternating DNA and π-conjugated sequences. Thermophilic foldable polymers, *J. Am. Chem. Soc. 125*, 5248−5249.
18. Saghatelian, A., Guckian, K. M., Thayer, D. A., and Ghadiri, M. R. (2003) DNA detection and signal amplification via an engineered allosteric enzyme, *J. Am. Chem. Soc. 125*, 344−345.
19. Prince, R. B., Barnes, S. A., and Moore, J. S. (2000) Foldamer-based molecular recognition, *J. Am. Chem. Soc. 122*, 2758−2762.
20. Wang, W., Li, L. S., Helms, G., Zhou, H. H., and Li, A. D. Q. (2003) To fold or to assemble? *J. Am. Chem. Soc. 125*, 1120−1121.
21. Gait, M. J. (1984) *Oligonucleotide Synthesis: A Practical Approach*, IRL Press, Washington, DC.
22. Hayakawa, Y., Kawai, R., Hirata, A., Sugimoto, J., Kataoka, M., Sakakura, A., Hirose, M., and Noyori, R. (2001) Acid/azole complexes as highly effective promoters in the synthesis of DNA and RNA oligomers via the phosphoramidite method, *J. Am. Chem. Soc. 123*, 8165−8176.
23. Amabilino, D. B., Ashton, P. R., Brown, C. L., Cordova, E., Godinez, L. A., Goodnow, T. T., Kaifer, A. E., Newton, S. P., Pietraszkiewicz, M., Philp, D., Raymo, F. M., Reder, A. S., Rutland, M. T., Slawin, A. M. Z., Spencer, N., Stoddart, J. F., and Williams, D. J. (1995) Molecular meccano. 2. Self-assembly of [ETA]catenanes, *J. Am. Chem. Soc. 117*, 1271−1293.
24. Letsinger, R. L., and Wu, T. F. (1995) Use of a stilbenedicarboxamide bridge in stabilizing, monitoring, and photochemically altering folded conformations of oligonucleotides, *J. Am. Chem. Soc. 117*, 7323−7328.
25. Lewis, F. D., Wu, T. F., Burch, E. L., Bassani, D. M., Yang, J. S., Schneider, S., Jager, W., and Letsinger, R. L. (1995) Hybrid oligonucleotides containing stilbene units: Excimer fluorescence and photodimerization, *J. Am. Chem. Soc. 117*, 8785−8792.
26. Ren, R. X. F., Chaudhuri, N. C., Paris, P. L., Rumney, S., and Kool, E. T. (1996) Naphthalene, phenanthrene, and pyrene as DNA base analogues: Synthesis, structure, and fluorescence in DNA, *J. Am. Chem. Soc. 118*, 7671−7678.
27. Berlin, K., Jain, R. K., Simon, M. D., and Richert, C. A. (1998) A porphyrin embedded in DNA, *J. Org. Chem. 63*, 1527−1535.
28. Bevers, S., O'Dea, T. P., and McLaughlin, L. W. (1998) Perylene- and naphthalene-based linkers for duplex and triplex stabilization, *J. Am. Chem. Soc. 120*, 11004−11005.
29. Rahe, N., Rinn, C., and Carell, T. (2003) Development of donor−acceptor modified DNA hairpins for the investigation of charge hopping kinetics in DNA, *Chem. Commun.*, 2120−2121.

BI050945Z